The Distribution of Boron between SiO_2–CaO–MgO Slags and Liquid Silicon at Controlled Oxygen and Nitrogen Potentials

Jesse WHITE[1], Carl ALLERTZ[2], Karl FORWALD[1], and Du SICHEN[2]*

[1]*Elkem Technology, 4675 Kristiansand, Norway*

[2]*Department of Materials Science and Engineering, Royal Institute of Technology, 100 44 Stockholm, Sweden*

Abstract: In the refining of solar-grade silicon using slag treatment, boron dissolved in the silicon is rejected to a liquid oxide (slag) phase. In this study the partitioning of boron between SiO_2–CaO–MgO slags and liquid silicon was examined at 1873 K over a range of slag compositions and gas compositions. It was found that the distribution of boron is dependent on the oxygen and nitrogen partial pressures as well as the slag composition. The highest partition ratios were achieved at 0.4 atm N_2 / 0.6 atm CO and below 55 mass % SiO_2. The concentration of MgO seems to have little impact on the partition ratio.

Key words: silicon refining, slag treatment, boron, oxygen, nitrogen

1. Introduction

Reinvigorated interest in renewable energy in recent years has led to an expansion in developing alternative, more inexpensive methods for refining of silicon to a suitable purity for use in solar panel manufacturing. Slag treatment is one refining technique that has been implemented on an industrial scale. Elkem Solar, the first commercialized operation [1] which utilizes slag treatment as part of the process chain, commenced production as recently as 2009. In this method, liquid silicon is brought into contact with a liquid oxide phase at high temperature and select impurities (mainly boron) in the silicon are rejected to the slag phase. The boron concentration in silicon can be reduced to very low levels.

Several researchers have measured the partitioning of boron between different slags and liquid silicon [2–4]. Unfortunately, the results are in substantial discordance, and most of the published studies were conducted at temperatures below industrial temperature ranges. Moreover, the values of boron partition ratios reported in the current body of available literature differ considerably from actual, typical values in the industrial slag refining process. Suzuki et al. [2] studied the effect of several different slags, including CaO–SiO_2 and CaO–MgO–SiO_2, from 1723 to 1823 K [2]. Silicon and slag were equilibrated in graphite crucibles for 2 hours under atmospheres of pure Ar, pure CO, and Ar/12.5 % CO_2. According to their results, the partition ratio of boron is a function of the slag composition, reaching a maximum at a CaO/SiO_2 ratio (basicity) of 0.7–1.0. Under a pure CO atmosphere, the maximum value of about 1.6 was attained with CaO–SiO_2–10% MgO slag. Teixeira and Morita [3] equilibrated silicon and various slags in graphite crucibles under argon atmosphere in an induction furnace at 1823 K. The duration of the experiments was 18 hours, which is considerably longer than Suzuki's experiments. They show L_B to be strongly affected by slag basicity, yet in contrast to the aforementioned study they show a distinct minimum value near a basicity of about 0.8–0.9. Johnston and Barati [4] conducted similar experiments equilibrating silicon and slags for 2 hours in magnesia or alumina crucibles in

a vertical tube furnace. The atmosphere was pure argon. Although the slag compositions were quite different (35 % Al_2O_3), the absolute values of L_B were similar to that of Suzuki et al. They sketch a dashed line showing the relationship of L_B to the slag basicity, indicating a maximum level at about a basicity of 0.6.

A comprehensive understanding of the thermodynamics of boron extraction is vital to advance the development of slag refining of silicon. The impetus of the present investigation was to clarify the effects of slag and atmosphere composition on the distribution of boron at a temperature relevant to industrial practice. In this investigation the oxygen potential of the gas was controlled at different levels via the C/CO equilibrium. Since the use of inert gas compositions is common industrial practice, the effect of the nitrogen potential was also studied. Considerably longer run times were employed (48 h) to ensure equilibrium.

2. Experimental

A gas/condensed phase equilibration technique was employed to study the distribution of boron between liquid silicon and slag over a range of slag compositions and varying gas compositions. The experimental method that was used is an “open circuit” technique as described in detail by Schwerdtfeger and Turkdogan [5]. In these experiments, the samples were contained in graphite crucibles and were flushed with binary gas mixtures of high-purity argon/nitrogen and carbon monoxide. A predetermined oxygen potential was imposed on the liquid silicon and slag by setting the concentration of CO in the inlet gas. The oxygen partial pressure in the system is governed by the reaction of CO (g) with graphite:

$$2\mathrm{C}(gr) + \mathrm{O}_2\ (g) = 2\mathrm{CO}(g) \tag{1}$$

$$\Delta G^{\circ}_{(1)} = -228\,800 - 171.5\,T\ (\text{joules})\ [6] \tag{2}$$

2.1. Experimental setup

The experimental apparatus is depicted in Figure 1. The setup is built around a vertical, electrical tube furnace with Kanthal Super heating elements and an alumina reaction tube (64 mm inner diameter). The reaction tube is sealed at its top by a brass, water-cooled quenching chamber. A water-cooled cap seals the bottom of the tube. The reaction gas enters the bottom of the tube and exits the quenching chamber on the top. A suspension rod fastened to a motorized screw drive is used to suspend the samples in the hot zone of the furnace. A Eurotherm controller sets and maintains the target furnace temperature. The control thermocouple is a Type B (Pt-6% Rh / Pt-30% Rh) thermocouple mounted in the wall of the furnace, which is positioned external to the reaction tube. The measurement thermocouple used in the tests is also Type B. A sapphire thermocouple sheath was used to protect the thermocouple against degradation from SiO (g) penetration. A gas train equipped with Bronkhorst analog mass flow meters and a mixing column filled with glass beads was used to meter the gas mixture into the reaction tube in the experiments.

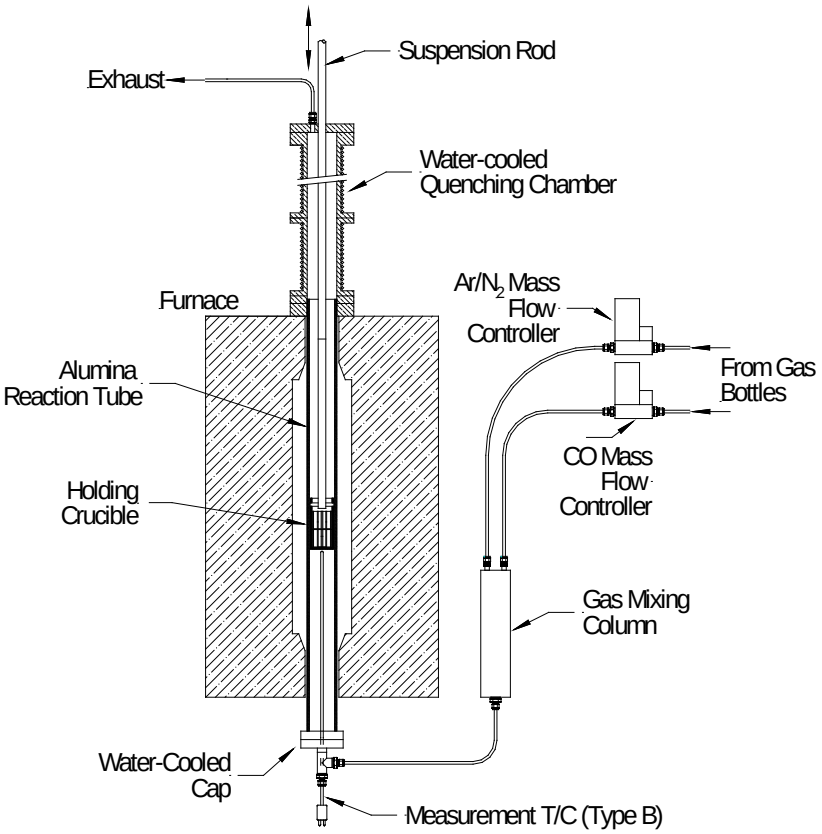

Fig. 1 Schematic of experimental apparatus used in this study

2.2. Materials preparation

Several different slag compositions were tested in each run at fixed gas compositions. A master eutectic $CaO–SiO_2$ slag was prepared at Elkem prior to the experiments, and was comprised of high-purity fused silica, and calcium oxide prepared by calcining precipitated calcium hydroxide. The composition of each slag sample was adjusted by blending small amounts of reagent-grade silica, calcium oxide, and magnesia with the master slag to achieve the desired slag compositions. Boron oxide was admixed with the slag constituents in the form of H_3BO_3. Higher concentrations of boron were used in this study compared to most of the previous investigations in order to facilitate more reliable chemical analyses. The equilibrium boron concentration levels were still well in the infinitely dilute range in both phases.

Up to 6 small graphite crucibles were prepared containing the silicon and slag constituents in varying proportions. The small crucibles, fabricated out of high-purity, isostatically-pressed graphite, had dimensions of 41 mm inner height and 18 mm inner diameter. The silicon used in this study was polycrystalline, electronic-grade purity. Large chips of silicon were placed in the bottom of the graphite crucible. The slag components were placed in each small crucible above the silicon chips. Each crucible contained 10 grams of slag components and 3 grams of silicon.

2.3. Experimental procedure

The small crucibles containing the samples were placed in a larger graphite holding crucible, fixed on a molybdenum tee on the tip of the suspension rod, and lowered into the center of the furnace. After lowering the holding crucible into position, the reaction tube was sealed, and the measurement thermocouple was positioned just below the holding crucible. The reaction tube was then evacuated and back-filled with argon several times. To commence the run, flow of reaction gas was commenced and the furnace controller was started. The temperature was ramped up to 1873 K at 4 degrees per minute. For the experiments conducted with CO–N_2 gas compositions, the reaction tube was flushed with pure argon gas up to the target temperature, and then switched over to the reaction gas composition in order to avoid nitride formation.

According to the CaO–SiO_2–MgO phase diagram, all the slag compositions were completely in the liquidus range at this temperature. The gas and condensed phases were equilibrated for 48 hours. At the end of the experiment, the holding crucible was rapidly drawn out of the furnace into the quenching chamber by action of raising the suspension rod with the motorized drive. A flow of argon gas into the quenching chamber was immediately initiated to facilitate quenching of the samples. The slag and silicon were separated, mechanically cleaned, and analyzed to measure the distribution of boron between the phases, and the resulting compositions of the slag samples.

2.4. Chemical analyses

All silicon samples were analyzed at Elkem Technology. The samples from Runs B1-2 through B6-3 were analyzed for boron using a Spectro ARCOS inductively coupled plasma optical emission spectrometry (ICP-OES) unit. For silicon Samples B8-1 through N3-3, analyses were conducted by atomic adsorption spectroscopy (AAS), using a Varian AA 280 FS. The estimated relative uncertainty for the ICP-OES and AAS analyses are ±5% and ±3%, respectively.

Slag Samples B1-2 to B11-6 were analyzed at an external laboratory using a Perkin-Elmer AAnalyst 300. The rest of the slag samples were analyzed at Elkem Technology using the aforementioned Varian AA 280 FS instrument. The estimated relative uncertainty for the slag analyses is given at ±5%.

For Samples N1-2 to N3-3, total nitrogen contents in the silicon and slag phases were quantified at Elkem Technology using a LECO TCH 600 instrument.

3. Results

The resulting equilibrium slag compositions and partition ratios of boron are presented in Tables 1 and 2. Table 1 lists the experiments conducted with CO–Ar gas mixtures, while Table 2 contains the results for the experiments using CO–N_2 gas mixtures. The oxygen partial pressures were calculated using Equation 2. Nearly all of the resulting equilibrium slag compositions are in the acidic range (> 50 mass % SiO_2). The boron partition ratio, L_B, is defined as the equilibrium mass ratio of boron in the slag to boron present in the silicon:

$$L_B = \frac{(\text{mass \% B})}{[\text{mass \% B}]} \tag{3}$$

where the oval brackets ( ) designate the liquid slag phase, and the square brackets [ ] designate the liquid silicon phase. In the slag refining of silicon, a high partition ratio is desirable (more boron rejected to the oxide phase). The values of L_B were directly determined from the chemical analyses. The final concentration levels of boron in this study are deemed to be well in the infinitely dilute range, since there is evidence to show that dilute solutions of boron in both liquid slag and silicon maintain Henrian behavior up to reasonably large concentrations [7].

Table 1 Experimental conditions and results of boron distribution experiments with CO–Ar mixtures at 1873 K

Sample No.	Inlet Gas		Equilibrium Slag Composition				Silicon	Partition Ratio, L_B	$\gamma_{(BO_{1.5})}$
	p_{CO} [atm]	p_{O_2} [atm]	SiO_2 [mass%]	CaO [mass%]	MgO [mass%]	B [mass%]	B [mass%]		
B1-2	1.0	4.6×10^{-16}	55.2	43.7	1.00	0.038	0.011	3.45	1.36
B1-3	1.0	4.6×10^{-16}	55.8	42.9	1.32	0.038	0.012	3.17	1.49
B2-1	1.0	4.6×10^{-16}	56.1	41.2	2.72	0.031	0.012	2.58	1.84
B2-2	1.0	4.6×10^{-16}	61.6	35.7	2.64	0.035	0.012	2.92	1.62
B2-3	1.0	4.6×10^{-16}	64.4	32.8	2.78	0.033	0.012	2.75	1.72
B3-1	1.0	4.6×10^{-16}	52.7	45.2	2.08	0.037	0.013	2.85	1.67
B3-2	1.0	4.6×10^{-16}	48.5	48.7	2.81	0.034	0.014	2.43	1.96
B3-3	1.0	4.6×10^{-16}	47.7	49.5	2.77	0.035	0.015	2.33	2.05
B4-1	1.0	4.6×10^{-16}	54.1	37.9	7.96	0.040	0.014	2.86	1.70
B4-2	1.0	4.6×10^{-16}	52.8	37.8	9.32	0.034	0.012	2.83	1.72
B4-3	1.0	4.6×10^{-16}	55.6	34.2	10.2	0.040	0.016	2.50	1.96
B5-1	1.0	4.6×10^{-16}	49.8	44.0	6.16	0.037	0.014	2.64	1.83
B5-2	1.0	4.6×10^{-16}	51.1	41.7	7.20	0.039	0.015	2.60	1.86
B5-3	1.0	4.6×10^{-16}	54.6	37.6	7.74	0.032	0.012	2.67	1.82
B6-1	1.0	4.6×10^{-16}	53.0	39.6	7.36	0.040	0.014	2.86	1.69
B6-2	1.0	4.6×10^{-16}	51.7	39.3	8.97	0.036	0.015	2.40	2.03
B6-3	1.0	4.6×10^{-16}	50.5	37.9	11.6	0.032	0.013	2.46	2.00
B8-1	1.0	4.6×10^{-16}	56.4	33.0	10.5	0.036	0.0141	2.55	1.91
B8-2	1.0	4.6×10^{-16}	54.0	33.8	12.1	0.042	0.0143	2.94	1.68
B8-3	1.0	4.6×10^{-16}	55.5	30.2	14.3	0.038	0.0136	2.79	1.78
B9-4	1.0	4.6×10^{-16}	58.1	30.8	11.1	0.027	0.0104	2.60	1.89
B10-1	0.8	2.9×10^{-16}	53.4	45.0	1.62	0.036	0.0134	2.69	1.26
B10-4	0.8	2.9×10^{-16}	58.3	39.1	2.62	0.036	0.0144	2.50	1.36
B10-5	0.8	2.9×10^{-16}	64.5	32.8	2.66	0.035	0.0140	2.50	1.35
B10-6	0.8	2.9×10^{-16}	65.8	31.2	3.01	0.034	0.0149	2.28	1.48
B11-1	0.6	1.6×10^{-16}	50.3	48.4	1.31	0.040	0.0146	2.74	0.80
B11-2	0.6	1.6×10^{-16}	50.2	48.1	1.61	0.039	0.0145	2.69	0.82
B11-3	0.6	1.6×10^{-16}	49.6	48.4	2.00	0.038	0.0156	2.44	0.91
B11-4	0.6	1.6×10^{-16}	54.0	43.3	2.63	0.044	0.0151	2.91	0.76
B11-5	0.6	1.6×10^{-16}	57.1	39.7	3.19	0.038	0.0162	2.35	0.94
B11-6	0.6	1.6×10^{-16}	56.4	39.9	3.77	0.037	0.0158	2.34	0.95

Table 2 Experimental conditions and results of boron distribution experiments with CO–N_2 mixtures at 1873 K

Sample No.	Inlet gas			Equilibrium Slag Composition					Silicon		Partition Ratio, L_B
	p_{N_2} [atm]	p_{CO} [atm]	p_{O_2} [atm]	SiO_2 [mass%]	CaO [mass%]	MgO [mass%]	B [mass%]	N [mass%]	B [mass%]	N [mass%]	
N1-2	0.10	0.90	3.7×10^{-16}	50.1	48.0	1.9	0.026	0.57	0.0075	0.0056	3.47
N1-3	0.10	0.90	3.7×10^{-16}	55.9	42.1	1.9	0.020	0.32	0.0082	0.0038	2.49
N1-5	0.10	0.90	3.7×10^{-16}	62.5	34.5	2.9	0.022	0.085	0.0078	0.0020	2.82
N1-6	0.10	0.90	3.7×10^{-16}	61.7	34.7	3.6	0.017	0.11	0.0065	0.0029	2.62
N2-1	0.20	0.80	2.9×10^{-16}	53.0	45.2	1.8	0.024	0.73	0.0065	0.0092	---
N2-2	0.20	0.80	2.9×10^{-16}	49.5	48.4	2.1	0.028	0.57	0.0057	0.0066	---
N2-3	0.20	0.80	2.9×10^{-16}	52.0	45.9	2.1	0.024	0.19	0.0080	0.0036	3.00
N2-4	0.20	0.80	2.9×10^{-16}	56.6	40.6	2.7	0.024	0.088	0.0084	0.0036	2.87
N2-5	0.20	0.80	2.9×10^{-16}	61.0	36.0	3.0	0.023	0.1	0.0079	0.0022	2.91
N2-6	0.20	0.80	2.9×10^{-16}	64.1	32.4	3.4	0.021	---	0.0087	0.0157	2.41
N3-1	0.40	0.60	1.6×10^{-16}	52.5	45.9	1.6	0.024	0.82	0.0076	0.0140	3.16
N3-2	0.40	0.60	1.6×10^{-16}	54.5	43.7	1.7	0.022	0.85	0.0069	0.0220	3.19
N3-3	0.40	0.60	1.6×10^{-16}	54.1	44.0	2.0	0.024	0.8	0.0072	0.0380	3.33

4. Discussion

It is conceivable that boron dissolved in molten silicon is oxidized and rejected to the slag phase and can be described by the reaction:

$$2\mathrm{B}\ (l) + \frac{3}{2}\mathrm{O_2}\ (g) = \mathrm{B_2O_3}\ (l) \tag{4}$$

To simplify calculations Equation 3 is recast as:

$$\mathrm{B}\ (l) + \frac{3}{4}\mathrm{O_2}\ (g) = \mathrm{BO_{1.5}}\ (l) \tag{5}$$

$$\Delta G^{\circ}_{(5)} = -664\ 630 + 127\ T \text{ (joules) [6]} \tag{6}$$

The standard states for the above reaction are pure liquid B, pure liquid $BO_{1.5}$, and 1 atm oxygen gas. The equilibrium constant is then written:

$$K_{(5)} = \frac{a_{\mathrm{BO}\ 1.5}}{a_{\mathrm{B}} \cdot p_{\mathrm{O_2}}^{3/4}} \tag{7}$$

Expanding and rearranging:

$$K_{(5)} = \left(\frac{\gamma_{\mathrm{BO}\ 1.5}}{\gamma_{\mathrm{B}}}\right)\left(\frac{X_{\mathrm{BO}\ 1.5}}{X_{\mathrm{B}}}\right)\left(p_{\mathrm{O_2}}^{-3/4}\right) \tag{8}$$

Since the mass ratio of boron, L_B, is directly proportional to the mole fraction ratio, then it follows that:

$$L_{\mathrm{B}} \propto K_{(5)} \cdot p_{\mathrm{O_2}}^{3/4} \cdot \left(\frac{\gamma_{\mathrm{B}}}{\gamma_{\mathrm{BO}\ 1.5}}\right) \tag{9}$$

For purpose of comparison with the literature, Figure 2 is a plot of L_B as a function of the CaO/SiO_2 ratio (basicity) of the slag. The values of L_B at 1 atm CO from the present work are shown here, and were categorized according to the MgO content in the slag. It is apparent that the results differ considerably from previously published studies.

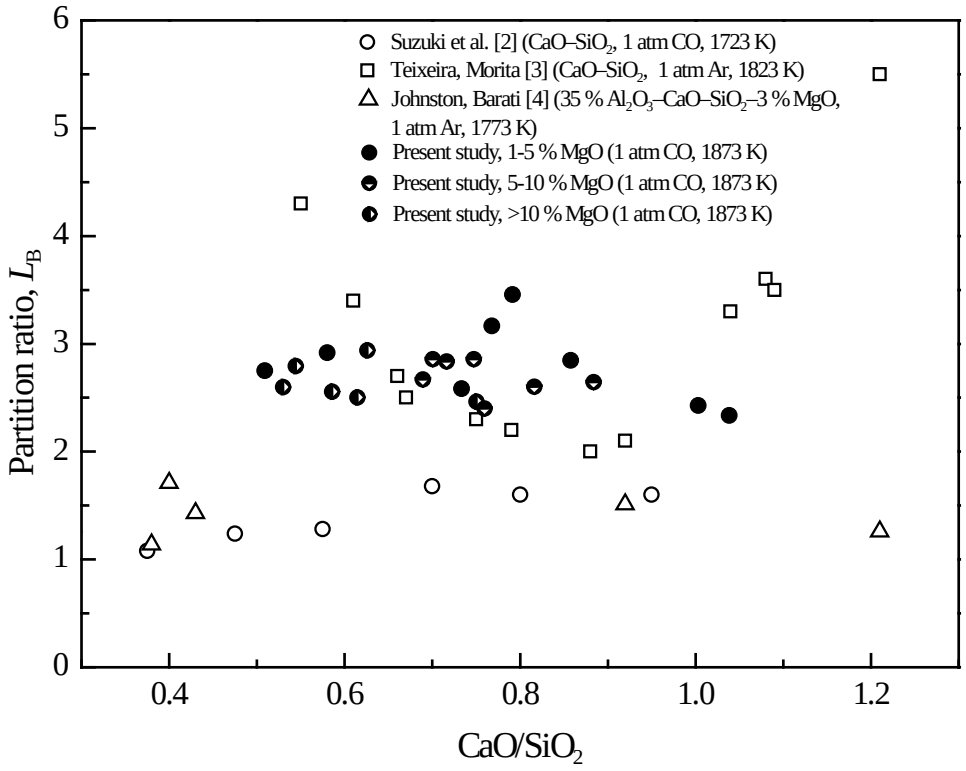

Fig. 2 The partition ratio of boron, L_B, as a function of the $CaO:SiO_2$ ratio in the slag, and comparison with previous studies

The values of Suzuki et al. [2] seen in Figure 2 were attained at 1 atm CO at a temperature of 1723 K. They show a maximum L_B of 1.6, which is considerably lower than the results of the present study. The lower temperature does not explain the lower L_B values compared to the present study: it is expected that the partition ratio would be greater at lower temperature, since the oxidation reaction of boron is exothermic (Equation 6), and thus the equilibrium constant should be larger in magnitude at lower temperature, which should increase L_B according to Equation 9.

Also shown in Figure 2 are the findings of Teixeira and Morita [3]. Their L_B values are in marked contrast to the other studies, and exhibit a much stronger dependence on the slag basicity as well as exhibiting a distinct minimum. Their values in the middle range of basicity agree reasonably well with the current study, but at both high and low basicities the L_B values are unreasonably large. Their highest reported value of L_B is about 5.5 at a basicity of 1.2.

Even though they studied quite different slag compositions, the data of Johnston and Barati [4] were included in Figure 2, since they did not use graphite crucibles, and they flushed with pure Ar in the experiments. Their reported L_B values are also considerably lower than the results of the present work.

Both Suzuki et al. and Johnston and Barati employed very short run times of 2 hours [2, 4], while Teixeira and Morita

[3] used equilibration times of 18 hours. According to our own experience from previous work, an equilibration time of at least 24 hours is necessary for this type of measurement. To ensure equilibrium with the gas phase, the present work employed a 48-hour run time. This may help explain the difference in our results as compared to the other studies.

4.1. Dependence of L_B on oxygen potential

The partition ratio of boron is likely dependent upon both the oxygen potential and the slag composition. The equilibrium slag compositions shifted somewhat from the ingoing compositions. Figure 3 is a plot of the dependence of L_B on the partial pressure of oxygen with constant slag composition. Figure 3 shows that at constant slag composition, L_B increases with increasing oxygen partial pressure for all three slag compositions. As also can be seen in this figure, the slag composition with the lowest SiO_2 content yields the highest partition ratios of boron.

The activity coefficient of boron oxide in the slag phase can be calculated by route of Equation 8. A reliable value for the activity coefficient of boron at infinite dilution in silicon, together with the current experimental data, is needed in order to calculate the activity coefficient of boron oxide. For the activity coefficient of boron at infinite dilution, γ_B°, the reported values in the literature [8–12] were compared. The most reliable data for the activity coefficient of boron at infinite dilution appears to be from Yoshikawa and Morita [12], who employed an equilibration technique with Si and BN in a Si_3N_4 crucible. Over the range of 1693–1923 K,

$$\log \gamma^\circ_{B(l)\text{in Si}(l)} = 126/T + 0.517 \quad (10)$$

The activity of boron in liquid silicon (with respect to liquid boron) deviates positively from Raoult's law. At 1873 K, γ_B° has a value of 3.84. The activity coefficients of boron oxide, $\gamma_{BO_{1.5}}$, with respect to pure liquid $BO_{1.5}$, are listed in Table 1. At 1 atm CO, the activity coefficient values range from 1.36 to 2.05. Further analysis reveals that the calculated $\gamma_{BO_{1.5}}$ increases with increasing oxygen partial pressure, which is unexpected. In these calculations, the interactions of boron with other solutes in the silicon present were neglected. However, in reality, Ca, Mg, and C are present in the silicon in significant quantities and should impact the activity coefficient of boron.

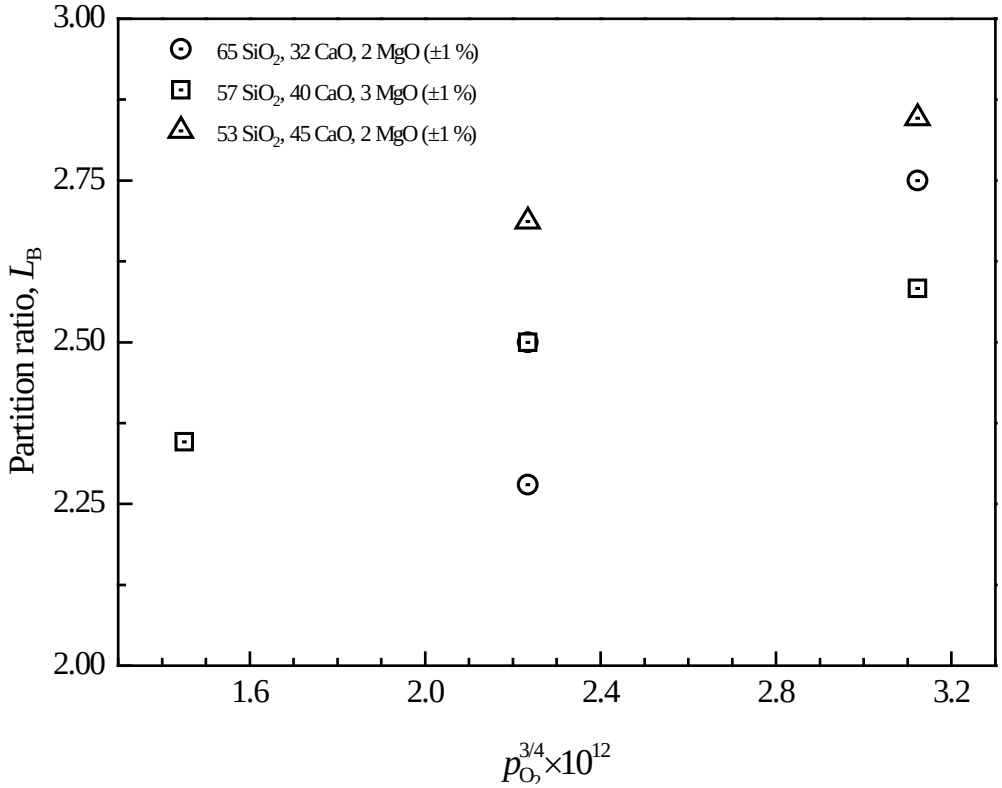

Fig. 3 The dependence of the partition ratio of boron on the oxygen partial pressure at 1873 K

4.2. Dependence of L_B on nitrogen potential

In the presence of nitrogen gas, it is reasonable to postulate that boron dissolved in molten silicon can be rejected to the slag phase following the reaction:

$$\mathrm{B}\ (l) + \tfrac{1}{2}\mathrm{N_2}\ (g) = \mathrm{BN}\ (l) \tag{11}$$

$$\Delta G^{\circ}_{(11)} = -300\,830 + 109.5\,T \text{ (joules) [6]} \tag{12}$$

Therefore, the partition ratio of boron should be dependent on the nitrogen capacity in the slag phase. A fair amount of research has been done concerning nitride dissolution in slags [13–17], mostly pertaining to steelmaking slags. The general consensus is that nitrogen dissolves in the slag according to the following reaction:

$$\tfrac{1}{2}\mathrm{N_2} + \tfrac{3}{2}\mathrm{O^{2-}} = \mathrm{N^{3-}} + \tfrac{3}{4}\mathrm{O_2} \tag{13}$$

Nitride capacity is defined as:

$$C_{\mathrm{N^{3-}}} = \frac{(\text{mass }\%\,\mathrm{N})\cdot p_{\mathrm{O_2}}^{3/4}}{p_{\mathrm{N_2}}^{1/2}} \tag{14}$$

The presence of carbon, as in the case of slag treatment of silicon (graphite crucibles) complicates matters. Nitrogen is also known to exist in slags as CN^- in significant concentrations, forming by the reaction:

$$\frac{1}{2}N_2 + C + \frac{1}{2}O^{2-} = CN^- + \frac{1}{4}O_2 \quad (15)$$

Therefore, the N^{3-} and CN^- concentrations in the slag should be related to both the free oxygen ion concentration in the slag (basicity), as well as the oxygen and nitrogen potentials.

Table 2 lists the boron partition ratios and the nitrogen concentrations in the silicon and slag phases for Runs N1–N3, which were conducted using N_2–CO gas mixtures, while Figure 4 shows the concentration of total nitrogen in the slag phase as related to the total nitrogen content in the silicon phase. The nitrogen concentration in the slag phase increases nearly linearly with increasing nitrogen content in the silicon up to about 0.6 mass %. Thereafter, the concentration in the slag phase levels out at about 0.85 mass %. This suggests that a saturation level of nitrogen in the slag is reached.

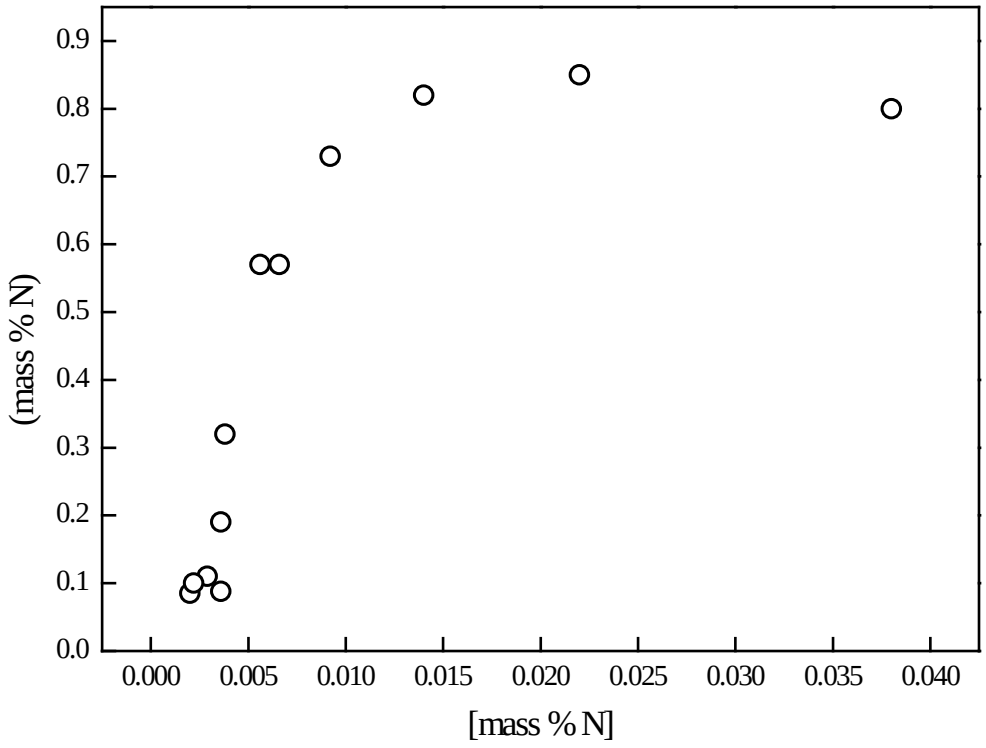

Fig. 4 The concentration of dissolved nitrogen in the slag related to the nitrogen concentration in the Si phase

Figure 5 is a plot of the partition ratio of boron with increasing nitrogen partial pressure. The partition ratio clearly increases with increasing nitrogen content in the gas. The highest partition ratios were reached at 0.4 atm N_2 (0.6 % CO) and the 53% SiO_2, 45% CaO and 2% MgO slag composition. The impact of slag composition on the distribution of boron can also clearly be seen from the figure. The fact that a high CO content combined with high N_2 content facilitates the greatest rejection of boron to the slag phase also leads to the conclusion that both Reactions (5) and (11) are occurring in parallel. Future experiments will investigate the effect of increasing N_2/CO ratios in the gas phase (up to $p_{N_2} = 1$).

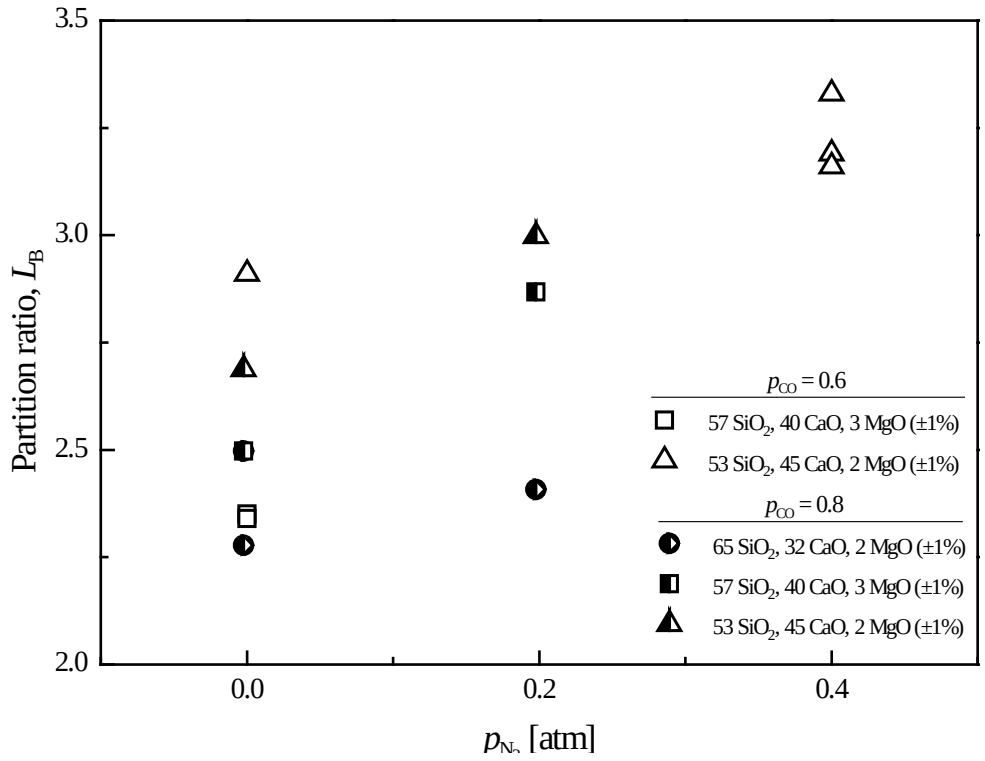

Fig. 5 The dependence of the partition ratio of boron on the nitrogen partial pressure at 1873 K

In light of this evidence, it makes little sense to calculate the activity of BN in the slag phase with the given data: boron is likely simultaneously associated with both oxygen and nitrogen in the slag phase. Making the assumption that the nitrogen in the slag is completely in the form of nitride, the capacity of nitride in the slag was calculated according to Equation 15. Figure 6 shows the nitride capacity as a function of the mole fraction of SiO_2 in the slag. The nitride capacity is seen to decrease with increasing silica content in the slag, which is expected given that the partition ratio of boron was found to be higher with lower silica content in the slag. The caveat, however, is that the fraction of the nitrogen dissolved in the slag in the form of CN^- is unknown, and could be substantial at low oxygen potential and carbon saturation. Therefore the relationship shown in Figure 6 should only be interpreted qualitatively.

These findings could prove to be valuable for the optimization of the industrial slag refining process. Firstly, the L_B values from this study are in much closer agreement with industrial boron partition values. The previous studies that were cited above have published values that are much lower than the normal partition ratio for boron in the industrial slag refining process. Secondly, it is evident that a fairly wide variance in the concentration of MgO in the slag can be tolerated without negatively impacting the partition ratio of boron. Finally, it has been confirmed that nitrogen can also play an active role in facilitating removal of boron from liquid silicon. The role of the gas composition should not be overlooked.

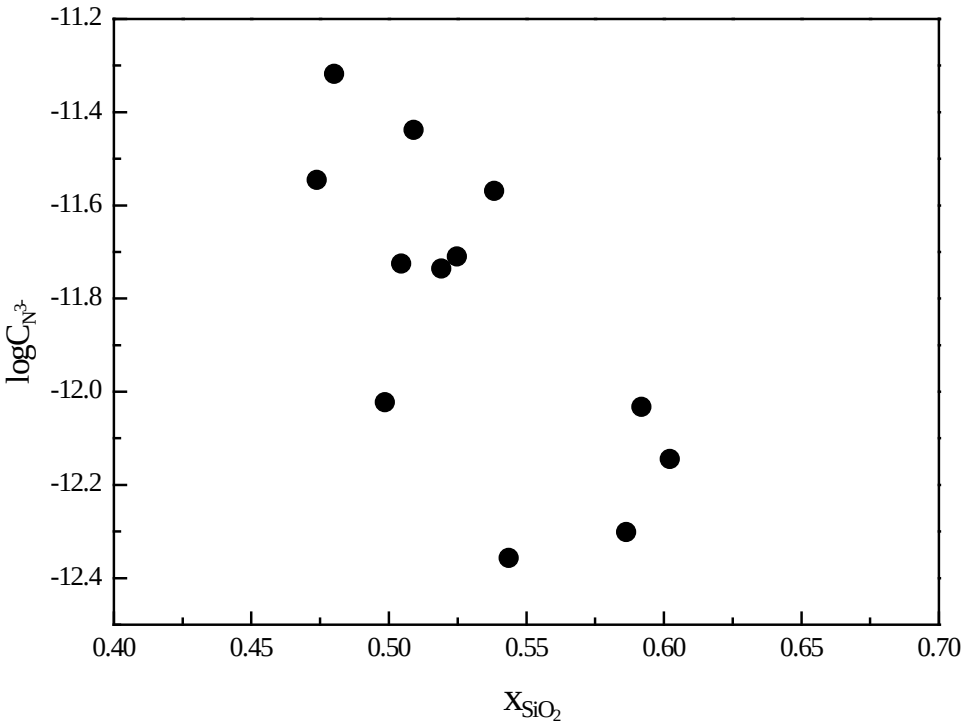

Fig. 6 The calculated nitride capacity as a function of the mole fraction of SiO_2 in the slag

5. Conclusions

The slag composition, the oxygen potential, and the nitrogen potential all have an influence on the distribution of boron between the silicon and oxide phases. The L_B values from this study are in fair agreement with the industrial process norms. With the current data, several conclusions can be made:

1. The highest boron partition ratios were achieved at 0.4 atm N_2 / 0.6 atm CO and below 55 mass % SiO_2.
2. A concentration of MgO of up to 15 mass % in the slag does not have a deleterious effect on the partition ratio of boron, which is advantageous for the industrial process.
3. Stabilization of the oxygen and nitrogen potentials in the furnace atmosphere is important for a consistent industrial process.

Acknowledgements

The authors wish to thank Elkem Technology and the National Research Council of Norway for their financial support.

References

[1] C. Zahedi, E. Enebakk, K. Friestad, M. G. Dolmen, J. Heide, T. Buseth, R. Tronstad, C. Dethloff. Solar Grade Silicon from Metallurgical Route. Technical Digest of the PVSEC-14, (Bangkok, Thailand), 2004.

[2] K. Suzuki, T. Sugiyama, K. Takano, N. Sano. Thermodynamics for Removal of Boron from Metallurgical Silicon by

Flux Treatment. *J. Japan Inst. Metals*, 1990, pp168-172.

[3] L. Teixeira, K. Morita. Boron Removal from Molten Silicon with Silicate Slag. Technical Digest of the PVSEC -17, (Fukuoka, Japan), 2007, pp87-88.

[4] M. D. Johnston and M. Barati. Distribution of impurity elements in slag-silicon Equilibria for oxidative refining of metallurgical silicon for solar cell applications. *Solar Energy Materials and Solar Cells*, 2010, 94, pp2085-2090.

[5] K. Schwerdtfeger, E. T. Turkdogan. Chapter 4B – Equilibria and Transport Phenomena Involving Gas Mixtures and Condensed Phases, Physicochemical Measurements in Metals Research, Part 1, R. A. Rapp (Ed.), Interscience Publishers, 1970, p348.

[6] E. T. Turkdogan. Physical Chemistry of High Temperature Technology, Academic Press, 1980.

[7] L. Teixeira, Y. Tokuda, T. Yoko, K. Morita. Behavior and State of Boron in $CaO–SiO_2$ Slags during Refining of Solar Grade Silicon. *ISIJ Int.*, 2009, 49(6), pp777-782.

[8] R. Noguchi, K. Suzuki, F. Tsukihashi, N. Sano. Thermodynamics of Boron in a Silicon Melt. *Metall. Trans. B*, 1994, 25B, pp903-907.

[9] M. Tanahashi, F. Toshiharu, Y. Chikabumi. Activity of Boron in Molten Silicon. *Shigen-to-Sozai*, 1998, 114(1), pp807-812.

[10] A. I. Zaitsev, A. A. Kodentsov. Thermodynamic Properties and Phase Equilibria in the Si-B System. *Journal of Phase Equilibria* , 2001, 22 (2), pp126-135.

[11] G. Inoue, T. Yoshikawa, K. Morita. Effect of Calcium on Thermodynamic Properties of Boron in Molten Silicon. *High Temp. Mat. and Proc.* 2003, 3–4(22), pp221-226.

[12] T. Yoshikawa, K. Morita. Thermodynamic Property of B in Molten Si and Phase Relations in the Si–Al–B System. *Mater. Trans. JIM* , 2005, 46, pp1335-1340.

[13] K. Schwerdtfeger, H. G. Schubert. Solubility of Nitrogen and Carbon in $CaO–Al_2O_3$ Melts in the Presence of Graphite. *Metall. Trans. B*, 1977, 8B, pp535-540.

[14] K. Ito, R. J. Fruehan. Thermodynamics of Nitrogen in $CaO–SiO_2–Al_2O_3$ Slags and Its Reaction with $Fe–C_{sat.}$ Melts. *Metall. Trans. B*, 1988, 19B, pp419-425.

[15] E. Martinez R., N. Sano. Nitrogen Solubility in $CaO–SiO_2$, $CaO–MgO–SiO_2$, and $BaO–MgO–SiO_2$ Melts. *Metall. Trans. B*, 1990, 21B, pp97-103.

[16] R. Inoue, H. Suito. Silicon–Oxygen Equilibrium and Nitrogen Distribution between $CaO–SiO_2$ Slags and Liquid Iron. *Metall. Trans. B*, 1992, 23B, pp613-621.

[17] I.-H. Jung. Thermodynamic Modeling of Gas Solubility in Molten Slags (I) – Carbon and Nitrogen. *ISIJ Int.*, 2006, 46(11), pp1577-1586.